Struct Multidisc Optim
DOI 10.1007/s00158-016-1563-6

RESEARCH PAPER

Topology optimization for heat conduction using generative design algorithms

Danny J. Lohan[1] · **Ercan M. Dede**[2] · **James T. Allison**[1]

Received: 5 November 2015 / Revised: 20 June 2016 / Accepted: 8 August 2016

Abstract In this article we present a new approach to topological design for steady-state heat conduction. The method capitalizes on the use of a generative algorithm to represent topology, resulting in a decrease in the number of variables in the design description. Using a generative algorithm as a design abstraction, the optimization technique is targeted to dendritic topologies that are known to perform well for heat conduction. Specifically, a traditional topology optimization technique (SIMP) is confirmed to produce branching characteristics in optimal designs. The Space Colonization Algorithm, which can generate similar topological patterns, is selected for in-depth investigation. A genetic algorithm drives generation of design candidates, providing a highly diversified search of the target design space. Finally, several synthesized optimal designs for steady-state heat conduction, derived using the described algorithms, are compared using commercial finite element software.

✉ Danny J. Lohan
dlohan2@illinois.edu

Ercan M. Dede
eric.dede@tema.toyota.com

James T. Allison
jtalliso@illinois.edu

[1] Department of Industrial and Enterprise Systems Engineering, University of Illinois at Urbana-Champaign, 117 Transportation Building, 104 S. Mathews Ave., Urbana, IL 61801, USA

[2] Electronics Research Department, Toyota Research Institute of North America, 1555 Woodridge Avenue, Ann Arbor, MI 48105, USA

Keywords Topology optimization · Generative algorithms · Conductive heat transfer

1 Introduction

Topology optimization has developed into an established research topic since the inception of the homogenization approach (Bendsoe and Kikuchi 1988). Though originally developed for structural mechanics applications, researchers have adapted the technique to steady-state heat conduction; see for example Bendsoe and Sigmund (2004), where a branching, 'tree-like,' structure is obtained using a two-dimensional (2-D) finite element framework. Gersborg-Hansen et al. (2006) used the finite volume method in conjunction with topology optimization to solve a similar planar heat conduction problem and observed that topology optimization for heat conduction produced designs similar to branching, 'five-finger' plans for optimal traffic patterns, where constant population density mimicked constant volumetric heating in a domain. Similar branching or dendritic characteristics still arise in 2-D structural design problems involving multiple objectives when a greater emphasis is placed on heat conduction, as demonstrated by de Kruijf et al. (2007). The planar heat conduction problem may also be solved using the level set method coupled with topological derivatives as in Zhuang et al. (2007), where multiple load cases were considered. Alternatively, evolutionary algorithms may be adopted for 2-D topology design of heat conducting fields, as discussed by Li et al. (2004). Extensions to three-dimensional (3-D) design for heat conduction, (Dede 2009; Chen et al. 2010; Burger FH et al. 2013), reveal that tree-like characteristics are not limited by the dimension of the solution space. In addition to isolated

Published online: 19 August 2016

heat conduction, heat conduction problems with convective boundary conditions have also been solved, (Bruns 2007; Iga et al. 2009; Yoon 2010; Dede et al. 2015). The combined conduction and convection problem also favors designs with tree-like structure. Thus, topology optimization has been successfully used to solve the steady-state heat conduction problem using an array of different computational algorithms, and the majority of studies confirm that dendritic topologies represent a class of optimal designs.

Regardless of the tendency of the reviewed methods to produce similar designs, it is well known that the efficiency and accuracy of structural topology optimization methods may be heavily dependent on the assumed starting material distribution, analysis mesh, and filtering techniques that are employed (Svanberg and Svard 2013; Sigmund and Maute 2013). Recent survey papers have presented comprehensive reviews of topology optimization developments, including an assessment of strengths and weaknesses across methodologies (Sigmund and Maute 2013; Deaton and RV 2014). Here an alternative approach to topology design is proposed through the use of generative algorithms. This approach is independent of the starting material distribution and mesh, and requires no filtering. Instead, generative algorithms are a class of recursive algorithms in which a low-dimension rule set can be followed iteratively to produce designs of higher dimension. Generative algorithms have shown promise in the topology optimization of truss structures (Khetan et al. 2015; Kicinger et al. 2005) through the efficient representation of large-scale topologies. By representing complex topologies efficiently, developing and evaluating complex designs becomes computationally efficient in an optimization procedure. This is possible since the design parameters are independent of the analysis mesh. This independence is a critical feature since computational expense is often dependent on the number of design variables, which scales linearly with mesh size for homogenization methods.

The specific contributions of this paper involve the demonstration of the generative design methodology from beginning to end. In doing so several key contributions are made, including: 1) selection criteria for choosing generative algorithms, 2) a novel method for rapid creation of unstructured body-fitted meshes, and 3) an investigation comparing topology optimization results with structured and unstructured meshes.

After introducing the problem formulation, results from a benchmark 2-D steady-state heat conduction topology optimization problem are presented to motivate the use of generative algorithms. A survey of generative algorithms is then provided. A specific algorithm is then selected for investigation via a series of studies that demonstrate its effectiveness for optimization under steady-state heat conduction. Optimal topologies are post-processed and corresponding final designs are synthesized for performance evaluation using commercial finite element analysis software. Findings and opportunities for future work are discussed in the conclusion.

2 Problem formulation

Here we consider the design of topology for steady-state, isotropic, heat conduction exclusively. This type of engineering system is relevant in modern electronics, where controlling the flow of heat through enhanced conduction to a predetermined heat sink location is critical to device temperature regulation. Consider a homogeneously heated design domain, as shown in Fig. 1. The design domain, Ω, is bounded by the solid black line. The temperature is fixed at zero on the Dirichlet boundary, Γ_D, represented by the dashed line. The Neumann boundary, Γ_N, is adiabatic and restricts heat flux out of the domain. The steady-state conductive heat transfer across the domain is represented by the following governing equations

$$\nabla \cdot (\kappa \nabla T) + f = 0 \text{ on } \Omega, \tag{1}$$

$$T = 0 \text{ on } \Gamma_D, \tag{2}$$

$$(\kappa \nabla T) \cdot \mathbf{n} = 0 \text{ on } \Gamma_N, \tag{3}$$

where T is the temperature state variable, f is the heat generated, and κ is the thermal conductivity of the material in the domain, Ω.

The benchmark design optimization problem considered here is to minimize the thermal compliance

$$\min_{\mathrm{x}} . \quad C(\mathrm{x}) = \int \nabla T (\kappa \nabla T) dA \tag{4}$$

$$\text{s. t.} \quad V(\mathrm{x}) = V_p \tag{5}$$

$$R(\mathrm{x}) \geq R_{\min}, \tag{6}$$

where the amount of conductive material, $V(\mathrm{x})$, is constrained to a prescribed value, V_p, and the radius of the conductive path, $R(\mathrm{x})$, must be larger than a prescribed value, $R_{\min}$. This constraint is used to enforce a minimum spacing constraint between thermally conductive sections to make the design manufacturable. The design vector, $\mathbf{x}$,

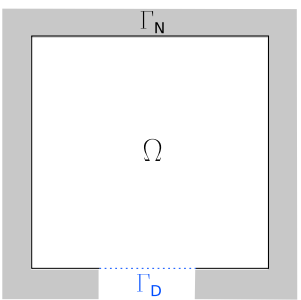

Fig. 1 Homogeneously heated design domain

consists of the design description, which is represented differently by the various algorithms implemented herein.

3 Optimal conductive heat transfer topological structure

Established topology optimization methods such as the Solid Isotropic Material with Penalization (SIMP) method (Bendsoe 1989; Bendsoe and Sigmund 2004) are capable of producing optimal designs without engineering intuition. The SIMP algorithm uses a design domain discretized into finite elements. Each element is assigned a continuous material amount, γ, that ranges from 0 to 1, representing void and solid material properties for the element, respectively. Singularities are avoided in solving the finite element problem by imposing a minimum material amount, often set to be $\gamma_{\min} = 0.001$, in each element. For the purpose of this study, each element is initialized with an equal amount of material such that the sum of the material on the domain equals V_P. A penalization factor of 2 is used to drive the material amount of each element towards a binary 0–1 distribution of material across the domain, and a density filter is used to enforce the minimum radius constraint equivalent to 1/20th of the domain width. The design algorithm is driven by the Method of Moving Asymptotes (MMA) optimizer, Svanberg (1987), which is compared with the Optimality Criteria (OC) algorithm. When using the SIMP method to solve the heat conduction problem, dendritic topologies such as the one presented in Fig. 2 (left side) typically result.

The optimal topology for steady-state heat conduction resembles the naturally occurring phenomena of *venation*, the arrangement of veins in a leaf; refer to the right-side image in Fig. 2. In heat transfer applications, numerous researchers have recognized the tendency of optimal topologies to resemble dendritic patterns that minimize the thermal resistance between heat source and heat sink, and they have capitalized on this basic principle in the development of optimization routines. Analogical design strategies (Lindsey et al. 2010; Chan et al. 2011) have been used to conduct more targeted design space searches. As a well-known example, Bejan et al. (2004) uses an approach similar to Lindenmayer-systems to develop tree-like structures that are optimal for conductive heat transfer. Bejan and Lorente (2006) also use similar observations from nature in developing algorithms that produce topologies for fluid flow systems. Salakij S et al. (2013) and Heymann et al. (2012) solve the topology design for convective heat transfer using an algorithm that generates fractal-like patterns directly. By developing a deep understanding about the physics underlying a given phenomenon, researchers are able use heuristics to develop targeted optimization tools. The focus of the remainder of this study is to identify and investigate a generative algorithm that may be used to generate topologies for steady-state conductive heat transfer as a basis for an efficient and flexible topology optimization method.

4 Generative algorithms

To perform a targeted search of the design space, a generative algorithm—also referred to as a generative design algorithm (GDA)—that efficiently produces complex dendritic structures must be identified. In this section, algorithms that have been developed to produce dendritic structures are explored.

4.1 Survey of generative algorithms

Several researchers in the computer graphics field have worked to efficiently and accurately reproduce leaf structures. Lindenmayer (1975) produced biological patterns using L-systems. Meinhardt (1976) produced dendritic structures using reaction diffusion models. Rodkaew et al. (2002) developed an algorithm based on particle systems which grew dendritic structures to an origin point. Runions et al. (2005) then adapted this algorithm to grow dendritic structures away from an origin point. Bejan and Lorente

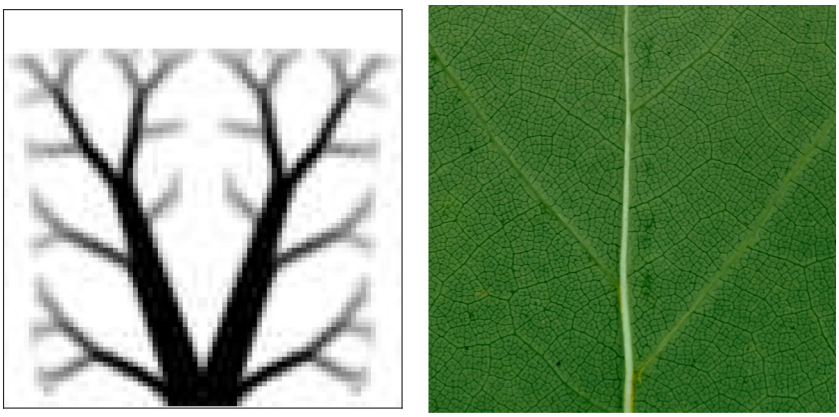

Fig. 2 Optimal heat conduction topology obtained using SIMP (*left*); note: dark colored regions = solid; light colored regions = void. Typical leaf vein patterns (*right*)

Table 1 Generative algorithm assessment

Basis	Generative algorithm	Design vars	Overlap	Boundary con.	Score key
Grammar	L-System; (Lindenmayer 1975)	△	×	×	◯ = Best
	Constructal Theory; (Bejan and Lorente 2006)	△	×	×	△
Interaction	Reaction Diffusion; (Meinhardt 1976)	◯	◯	◯	× = Worst
	Particle System; (Rodkaew et al. 2002)	◯	◯	◯	
	Space Colonization; (Runions et al. 2005)	◯	◯	◯	
Physics	Erosion Model; (Errera and Bejan 1998)	×	◯	◯	
	SIMP; (Bendsoe 1989)	×	◯	◯	

(2006) developed constructal theory to produce dendritic structures for heat and mass transfer problems. Table 1 summarizes candidate algorithms for use in topology optimization of heat conduction systems. The algorithms have been divided into three groups based on common themes. The L-System and Constructal Theory algorithms are 'Grammar-Based' and use rules to both define components and guide their assembly. The Reaction Diffusion, Particle System, and Space Colonization algorithms are considered 'Interaction-Based,' where only the rules governing interactions are controlled. The Erosion Model (Errera and Bejan 1998) and SIMP (Bendsoe 1989) techniques may also be considered 'Physics-Based' generative algorithms as they evolve parameters over time based on their respective physics-based criteria. Material distribution strategy is the core distinction between these two methods; the Erosion Model adds material to the domain, whereas the SIMP procedure redistributes a given amount of material across the domain. The groupings of the algorithms are set according to the specific form of each algorithm, and it is noted that modifications may be made to address the weakness of each algorithm.

The algorithms are assessed qualitatively based on criteria that correlate to efficient use in structural topology optimization, including: the number of design variables, whether topology overlaps, and whether the algorithm produces a topology that is restricted to the feasible design domain. The scoring system is based on relative differences between the alternate algorithms. At a glance, the 'Grammar' based algorithms seem to require additional rules to satisfy the design requirements for the heat conduction problem. The 'Interaction' based algorithms have the lowest number of design variables and represent designs efficiently with a limited number of parameters. Both the 'Interaction' and 'Physics' based algorithms inherently prevent topology overlap and satisfy boundary conditions; although with the latter category, the number of design variables may quickly become excessive due to the design variable representation. Thus, using the selected criteria, the 'Interaction' based algorithms appear to most easily satisfy the requirements for a compact, realistic, and feasible model. Between the three interaction based algorithms, the Space Colonization algorithm is selected for use based on the explanation in the following section.

4.2 Space colonization algorithm

The Space Colonization algorithm follows the *canalization hypothesis*, (Sachs 1981), which suggests that leaf veins grow towards hormone centers, called auxins, located throughout the leaf. The space colonization algorithm mirrors this procedure to produce realistic looking leaves and other dendritic structures efficiently (Runions et al. 2005). The algorithm begins from a source node or initial stem, **v**, shown in green, Fig. 3. A set of auxins, **S**, are then introduced on the design domain, shown in blue. Each auxin, **s**,

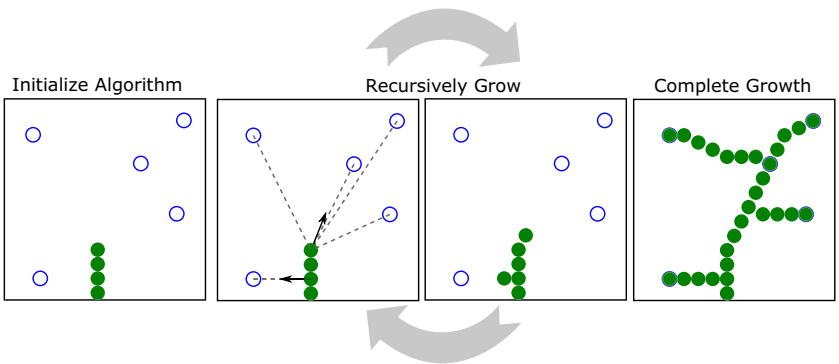

Fig. 3 Space colonization algorithm growth procedure. Note: *blue* colored open circles indicate auxins; *green* fully colored circles indicate vein nodes

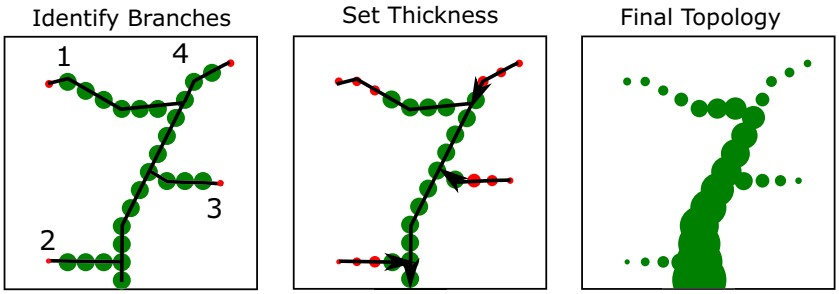

Fig. 4 Space colonization algorithm thickness assignment procedure. In this example, the thickness is defined by the radius of the circle. Note: *green* fully-colored circles indicate vein nodes

is then paired with the nearest vein node. The vein node proceeds to grow in the average direction, $\mathbf{n}$, of its paired auxins by a fixed step, D.

$$\mathbf{v}' = \mathbf{v} + D\frac{\mathbf{n}}{||\mathbf{n}||}, \text{ where } \mathbf{n} = \sum_{\mathbf{s}\in\mathbf{S}(\mathbf{v})} \frac{\mathbf{s}-\mathbf{v}}{||\mathbf{s}-\mathbf{v}||} \tag{7}$$

The algorithm grows recursively until all auxins have been reached by a vein node. Upon completion of growth, the branches are identified and ordered from longest to shortest. The extremities of each branch are then set to a minimum thickness and the vein nodes linearly increase in size from extremity to source node. Note that other non-linear sizing approaches may also be implemented. The final node location and thickness information can be used along with graphical tools to generate 2-D and 3-D leaf-like branching patterns; refer to Fig. 4 for a graphical description.

The process whereby the algorithm grows towards auxins intuitively translates to a heat transfer framework where cooling passages would grow towards heating elements.

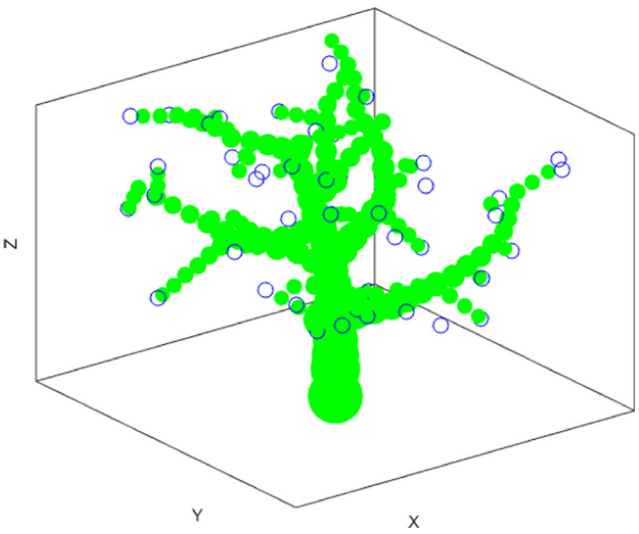

Fig. 5 Space colonization algorithm in 3D. The thickness parameter here is defined by the radius of a uniform sphere

For this reason, the Space Colonization algorithm was chosen for further development. When scaling the algorithm to three dimensions, the design vector increases in size by one half the length of the original design vector (Runions et al. 2007). This small increase in design vector size allows for an efficient search of three-dimensional designs. One such three-dimensional structure is presented in Fig. 5. The complexity of the final design may be increased by various methods. One strategy is to introduce additional auxins on the design domain. Another is to introduce the auxins at different intervals during the algorithm growth. This promotes the development of secondary and tertiary branching structures, as shown in Fig. 6. Highly dendritic structures may then be produced using as few as two dozen design variables.

4.3 Space colonization in optimization

With the goal of performing a diversified search for optimal designs, a genetic algorithm (GA) is used to drive the optimization procedure. The GA was implemented using the MATLAB® global optimization toolbox. The conductive material topology is represented as a vector, $\mathbf{a}$, of real numbers, the genotype, which correspond to the x and y coordinates of the n auxins:

$$\mathbf{a} = \left[\, a_{1x},\ a_{1y},\ a_{2x},\ a_{2y},\ \cdots,\ a_{nx},\ a_{ny} \,\right]. \tag{8}$$

By operating on the indirect representation of the topology, the dimension of the design problem is reduced significantly, thus increasing the efficiency of design space exploration. The genotype is converted to the phenotype representation, i.e. the topology, through the space colonization algorithm, after which design performance can be evaluated (Fig. 7). Due to the population-based nature of GAs, multiple design evaluations may be performed in parallel to improve computational efficiency. Other gradient-free optimization algorithms may be viable. Using a generative design algorithm (GDA) as a design abstraction to map low-dimension optimization variables to a detailed design representation, in conjunction with an outer-loop optimization algorithm, will be referred to here as a generative design

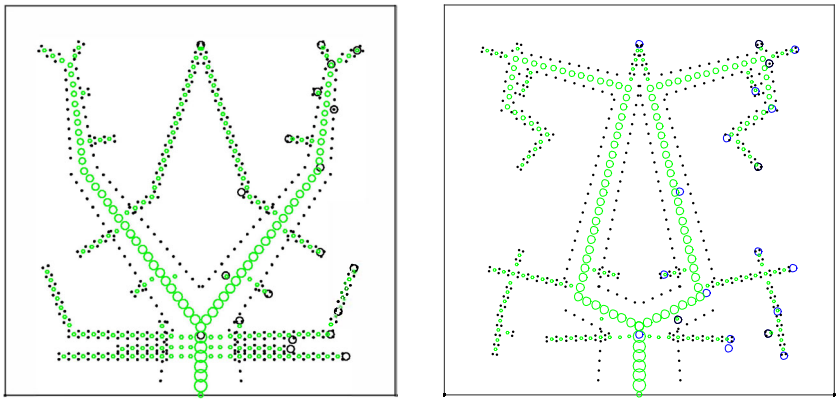

Fig. 6 Branching topology created using 20 auxins (*left*). Branching topology created using 20 auxins introduced at intervals (*right*)

methodology (GDM). A flowchart of a GDM based on a GA outer loop is illustrated in Fig. 8.

To explore the effect of design complexity on performance, a study was conducted that varied the number of auxins and development stages. The compliance objective was evaluated across a regular 400x400 mesh. The GA was initialized with a random population (size 10) for 100 generations. The results reported in Fig. 9 are the best of 10 trials using the GA.

From this initial study several observations can be made. Analyzing the first development stage experiments, the objective function decreases towards 30 auxins, then increases as auxins number increases. Analyzing the optimized topological structures from this study, it was observed that highly dendritic structures result in a greater average temperature across the domain, hence increasing the compliance objective. A similar trend was seen using the SIMP method when varying the minimum radius constraint between optimization routines. When observing the performance of the 2- and 3-development stage curves, the optimal designs saturate near a compliance value of 2000. This is due to the ability of the multi-stage approach to place auxins on top of each other and hence produce less dendritic structures that satisfy all constraints (similar to those with 30 auxins). To produce designs similar to those achieved with SIMP, 20 auxins will be used in all subsequent studies.

5 Meshing and analysis independence of design representation

One important motivation for using a GDA as a design abstraction is to separate design representation from analysis mesh. In addition to providing a low-dimension parameterization, this abstraction supports more efficient and accurate analysis meshes (but requires mesh construction for each new design candidate). This section presents a method for evaluating designs obtained via the GDA with an emphasis on understanding computational expense. To compare fairly the GDM with SIMP, both algorithms are evaluated using the same finite element solver. In each case, the square design domain from Fig. 1 is discretized using a regularized mesh (RM) with equally sized quadrilateral finite elements. The space colonization algorithm is modified slightly to produce designs comparable to those obtained using the SIMP method. Specifically, each node at an extremity of the topology is set to the same R_{min} value used in the SIMP algorithm to satisfy the minimum radius constraint. To satisfy the solid material volume constraint, an optimization routine is executed to uniformly scale the thickness of all nodes. From there, the space colonization algorithm is mapped onto the discretized design domain via projection using the locations of the discretized nodes and their respective node thickness, as illustrated in Fig. 10. Solid material

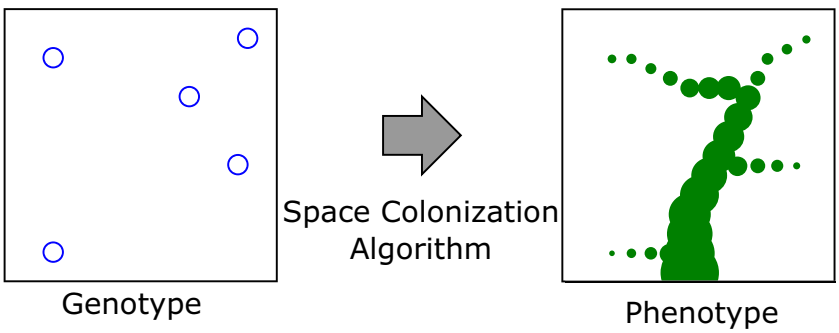

Fig. 7 Genotype to phenotype mapping

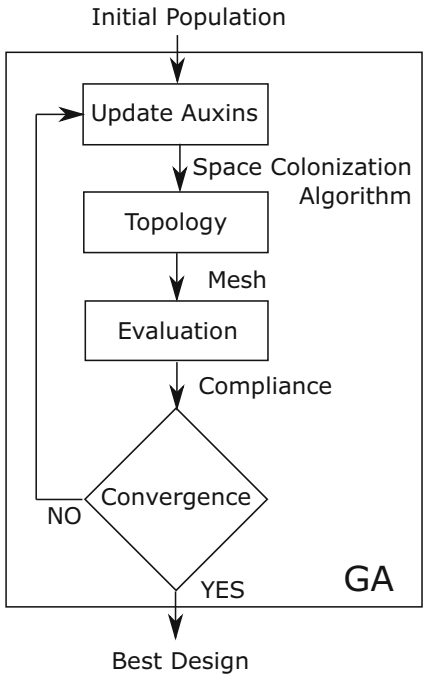

Fig. 8 Flowchart of computations for generative design methodology (GDM)

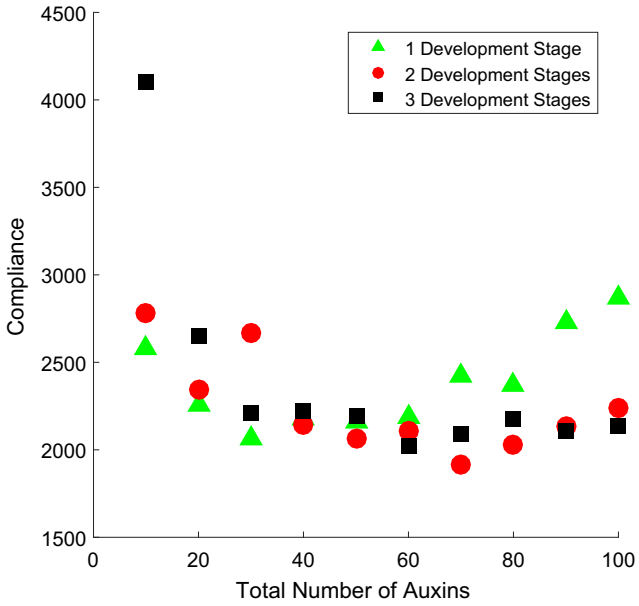

Fig. 9 Design complexity experiments

properties are assigned to finite elements whose element centers lie within the prescribed radius of a vein node.

For straightforward comparison with the GDM, a simple threshold is applied to the final output of the SIMP algorithm to obtain a domain with similarly-well defined, i.e., 0–1, material properties. If the material amount, γ, is above a given threshold, m_T, the finite element property is set to unity. Otherwise, the material property is set to zero. To ensure the solid material volume fraction is satisfied within tolerance, Newton's Method is used to determine the proper threshold, m_T, value. Figure 11 demonstrates the change in the topology obtained using SIMP when applying a threshold filter.

Though the topology on the right in Fig. 11 does not satisfy the minimum radius constraint, it consists of only void and solid material. The grayscale topology on the left in Fig. 11 has an objective function (i.e. thermal compliance) value of 1706, while the threshold filtered topology on the right in Fig. 11 has a thermal compliance value of 2320.

5.1 Numerical results

To compare the computational expense of the algorithms with respect to analysis mesh size, both algorithms are set to terminate by convergence, specified as a change of compliance less than 1 %, or a 100 function evaluation limit. The GDM is set to use a GA population size of 10 with nine generations to result in a total of 100 evaluations. Similarly, the SIMP algorithm is set to perform up to 100 evaluations. The results of this numerical study are presented in Fig. 12.

The GDM is observed to perform well when increasing the analysis mesh resolution. By using a gradient-free method to drive the optimization, the expensive task of calculating sensitivities for a dense mesh is avoided. However, achieving convergence using the GA requires many more iterations. Figure 13 demonstrates the convergence of the GDM fitness value as a function of GA generation. Given that the topology is an approximation which needs manual post processing, complete convergence may not necessarily represent the final design, (Brackett et al. 2011). An alternative strategy for using topology optimization in design efforts is to generate and evaluate different topologies for brainstorming purposes (convergence is not necessary in this case).

6 Design space exploration results

The generative nature of the space colonization algorithm supports a diverse search of the design space. A small perturbation in design variables may cause drastic changes in the resultant topology as the auxin locations do not directly define where the vein will grow from the base. By using this indirect design representation with a small number of design variables, a limited number of experiments may produce a large variety of designs. Figure 14 demonstrates the variety of topologies that are explored within 100 computational iterations using both the SIMP (left image) and the GDM (right image) algorithm. In this example, the SIMP

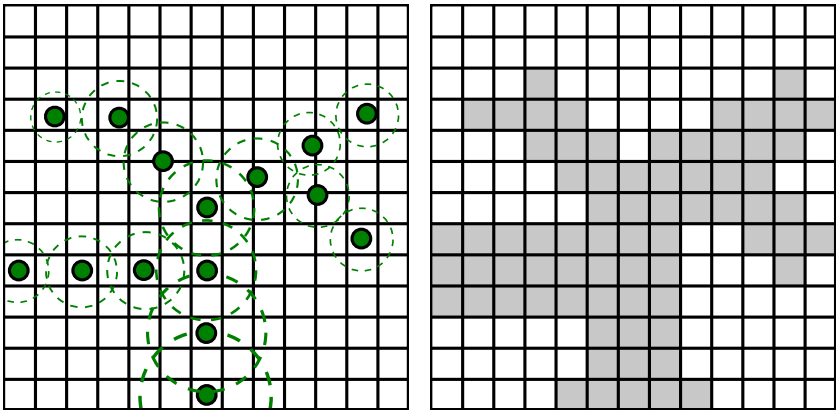

Fig. 10 Generative algorithm mapping demonstration. The image on the left shows the node locations as green fully-colored circles with associated material diameter as concentric *dashed circles*. The image on the right shows the mapped topology, where gray colored elements indicate solid material and white colored elements indicate void

algorithm begins with a uniform material distribution throughout the domain. The material is then iteratively redistributed throughout the structure until convergence to an optimal design. The SIMP algorithm initially evaluates designs that are not well defined (i.e. have significant amounts of gray material), and near convergence samples nearly identical designs. This is due to the homogeneous material distribution at the start, and decrease in optimization step size near the optimal solution.

SIMP is a powerful tool in terms of rapid convergence toward a local optimum, but exhibits limited design space coverage. In contrast, the GDM takes a different approach where convergence or optimality will not likely be achieved within the 100 function evaluation limit. The generative design algorithm, however, evaluates 100 distinctly different designs during the optimization routine. This is done by sampling 10 unique designs within the dendritic structure design space to evaluate and modify within the maximum number of function evaluations. As a result, the GDM exhibits broader design space coverage than SIMP.

It is clear from Fig. 14 that the GDM tests a wide variety of dendritic structures through the use of the space colonization algorithm. For the purpose of numerical comparison, two structures have been selected for further investigation, as shown in Fig. 15. The GDM RM 1 structure was observed to have a thermal compliance value of 1687, while the GDM RM 2 design has a thermal compliance value of 1850.

Though both the SIMP and GDM strategies are efficient at searching for candidate optimal topologies, the design algorithms are restricted by the resolution of the candidate mesh. To obtain a more accurate evaluation of a given candidate topology, strategies for obtaining and evaluating topological designs using an explicit boundary representation are explored.

7 Body-fitted mesh

The GDM outputs node locations that are interpolated to obtain an explicit representation of the topology. To capitalize on the availability of an explicit boundary representation, a body-fitted (BF) meshing technique must be adopted. Given such an intricate topology, meshing for use with a finite element solver becomes a challenge. This is due to the requirement of meshing two discrete bodies together. Mesh generation techniques such as Polygonal meshing, (Talischi et al. 2012), are capable of producing meshes within a closed body. This technique, however, falls short of requirements when the two bodies must be combined, resulting in a non-conforming mesh, shown in Fig. 16.

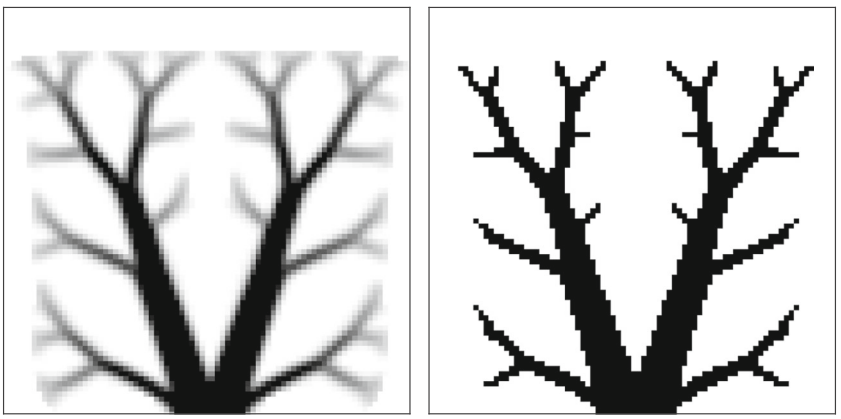

Fig. 11 Application of threshold filter to obtain pure 0–1 designs from the SIMP result. Note: dark colored regions = solid; light colored regions = void

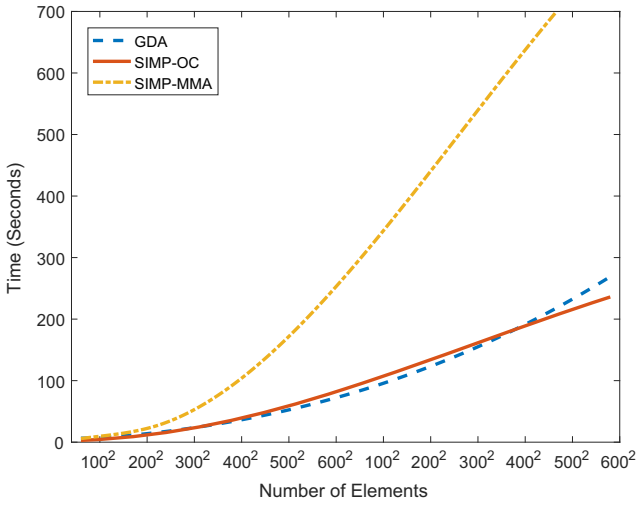

Fig. 12 Computational expense comparison using a 3.47 GHz processor with 48 GB RAM running Windows XP

A solution to this issue is to combine the two meshes together, but this technique is computationally expensive. For this reason, attention is turned to mesh refinement techniques. Mesh refinement techniques that start with a square grid, such as a 'cookie' cutter approach (Biabanaki and Khoei 2012; Biabanaki et al. 2014), or element-wise mesh refinement (Sarhangi Fard et al. 2012), demonstrate a capability for meshing the dendritic topology. Though these techniques are effective in approximating a geometry, they still rely heavily on a grid of square finite elements. An alternative approach for explicit representation of topology using triangular elements was successfully proposed for topology optimization by Christiansen et al. (2014). The authors noted, however, that when used with topology optimization, the meshing technique is computationally expensive. These challenges motivated the development of a new meshing strategy.

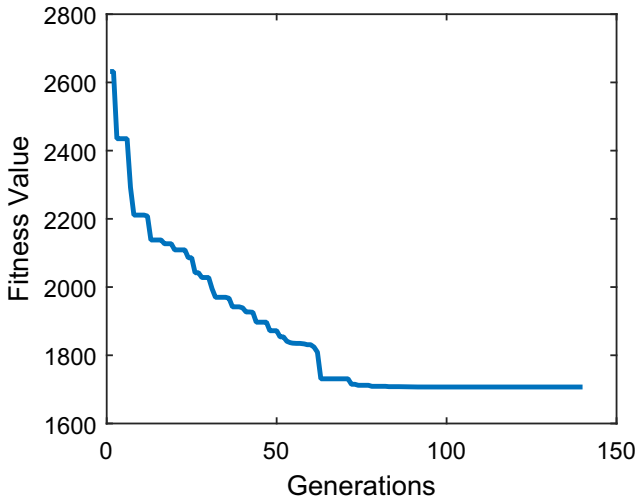

Fig. 13 Convergence of GDM as a function of GA generation

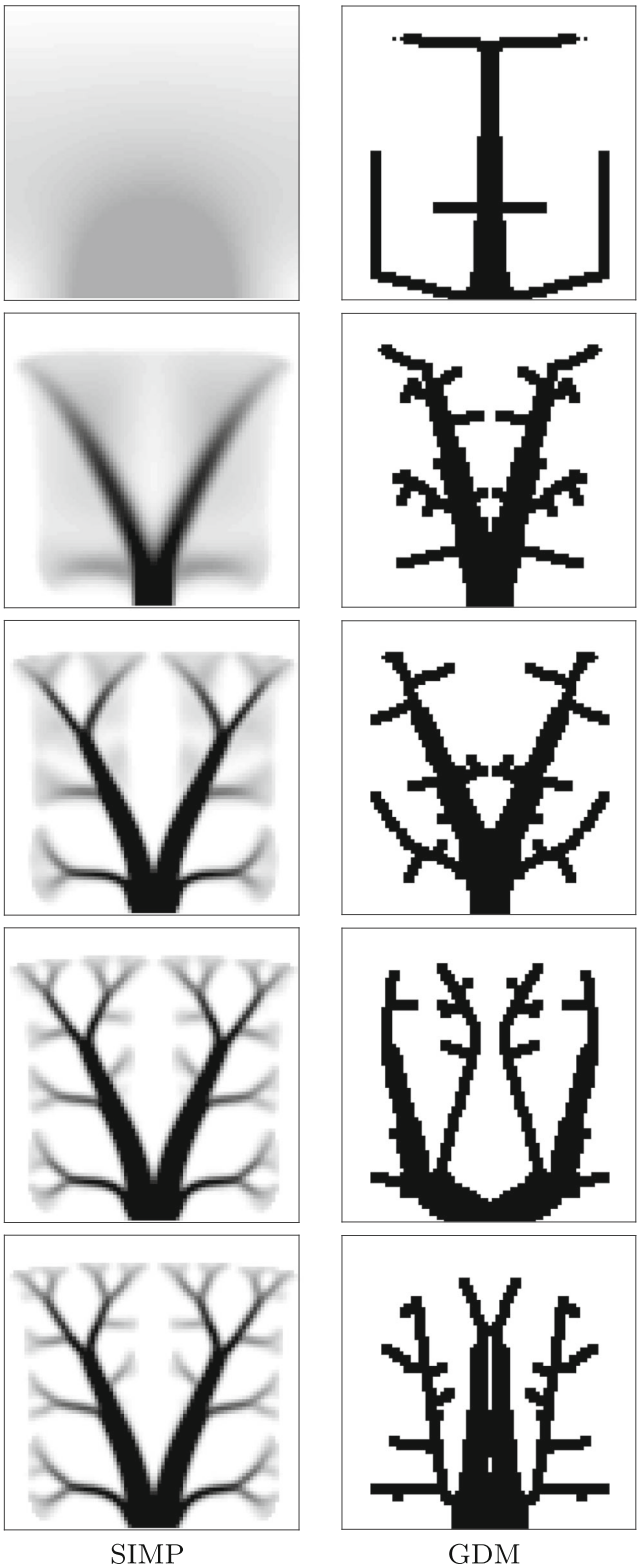

Fig. 14 Design diversity via alternative algorithms

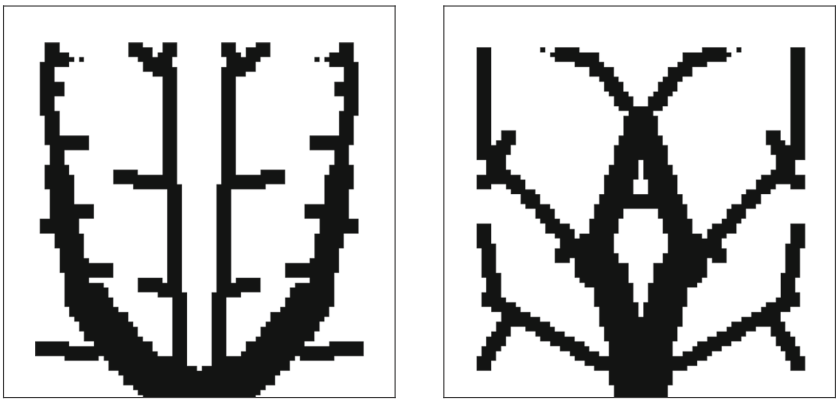

(a) GDM RM 1 (b) GDM RM 2

Fig. 15 Candidate optimal designs from GDM on a regular mesh (RM)

The meshing technique is inspired by force-directed graph drawing, which was first developed by Fruchterman and Reingold (1991). Force-directed layout has been used to untangle existing meshes (Bowmick and Shontz 2010; Nitin 2012), but to the authors' knowledge, never for mesh generation. The proposed algorithm combines force direction with particle generation to produce point clouds with a high density near domain boundaries, thereby reducing the need to iterate for accuracy. Details describing the implementation of the algorithm follow.

7.1 Force-directed meshing

The force-directed meshing algorithm uses discrete information from the space colonization algorithm output as a basis for the mesh. The meshing procedure begins by introducing particles, shown in red, placed uniformly across the design domain (Fig. 17a). Each particle is paired with its nearest vein boundary node, shown in black. Each particle experiences a force directing it towards its paired vein boundary node:

$$\mathbf{F}_{\mathbf{p}_i} \propto \frac{1}{|\mathbf{p}_i - \mathbf{b}_n|}\left(\frac{\mathbf{p}_i - \mathbf{b}_n}{|\mathbf{p}_i - \mathbf{b}_n|}\right) \tag{9}$$

where the magnitude of the force experienced by a mesh particle node, $\mathbf{p}_i$, is proportional to the inverse of the distance between the given particle node and its nearest vein boundary node, $\mathbf{b}_n$. The particles are simulated for a few time steps using forward Euler method allowing them to tend towards the domain and topology boundary:

$$\mathbf{p}[t_{k+1}] = \mathbf{p}[t_k] + h\mathbf{F}_{\mathbf{p}}[t_k] \tag{10}$$

where k is the current time step and h is a discrete step in time. Particles that are within a tolerance radius of the boundary are 'frozen' from motion (Fig. 17b). 'Freezing' particles promotes a high particle distribution near boundaries and reduces the computational expense of the simulation by removing the particles from calculation. At the final time step, a new set of particles are introduced uniformly across the domain (Fig. 17c). This enforces a minimum element size when creating a mesh. After a specified number of particle generation phases, the point cloud information is then passed to a Delaunay triangulation function in MATLAB®, `delaunay`, to produce a triangular mesh, as shown in Fig. 17d.

With an explicit boundary defined for the topology, material properties are assigned to each element via projection

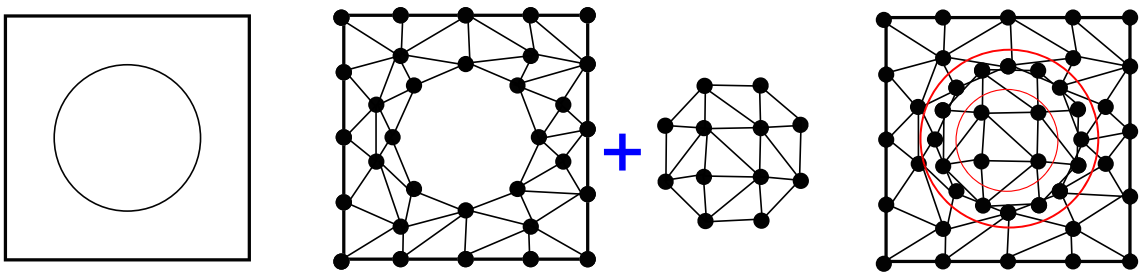

Fig. 16 Body combination resulting in a non-conforming mesh

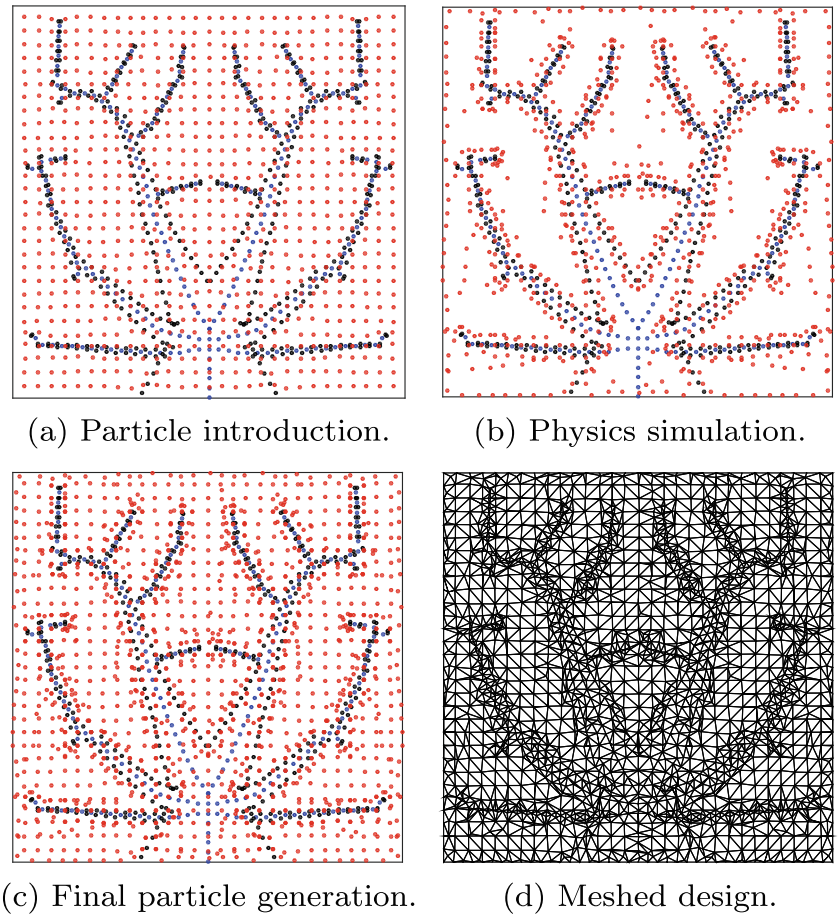

Fig. 17 Force-directed BF meshing sequence

on a triangular grid (Fig. 18). If a node of a triangular element lies within a radius defined by the thickness of the vein node, the triangular element is assigned conductive material properties.

7.2 Numerical results

Using a BF mesh requires re-meshing, which increases computational cost. Yet, due to approximately smooth boundaries, this design is closer to a manufacturable part. Using a GA with 100 evaluations, a population size of 10, iterated over nine generations, the topologies in Fig. 19 were produced.

The topologies presented were obtained by the same optimization routine performed twice. The topology on the left had a thermal compliance value of 2049 and the topology on the right had a thermal compliance of 2345. Though one topology has a clear advantage in compliance, both topologies are presented as they are distinct in their structure. These two designs are presented as an example of the GDM's ability to explore a wide variety of topologies.

8 Comparison via high-fidelity analysis

To compare fairly the SIMP OC, SIMP MMA, GDM RM, and GDM BF design algorithms (binary material distribution, smooth boundaries, equal volume fraction), the respective topologies were imported into an open-source vector

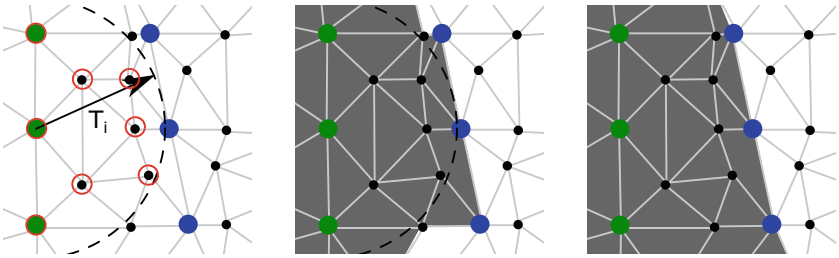

Fig. 18 Nodes that lie within T_i are identified in red (*left*). Material properties are assigned to all elements adjacent to red nodes (*center*). Material assignment fully carried out (*right*)

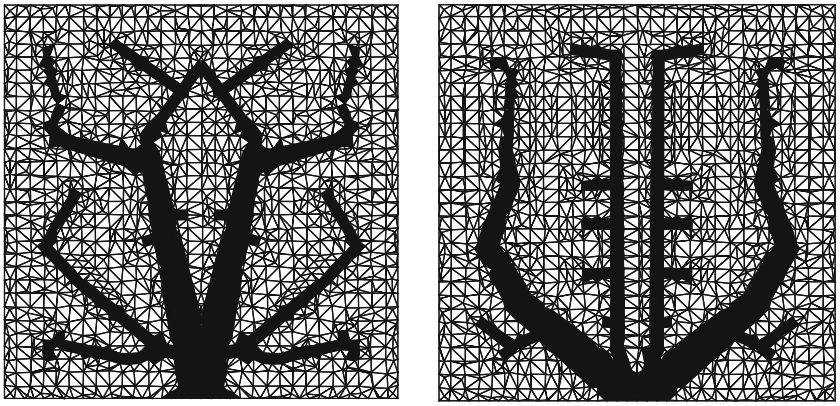

(a) GDM BF 1 (b) GDM BF 2

Fig. 19 Body-fitted mesh topology

graphics editor, *Inkscape*,[1] where standard image processing tools were used to create explicit vector representations of each design. The spline representations were imported into a commercial finite element analysis (FEA) package, COMSOL Multiphysics, to evaluate conductive heat transfer performance. Uniform heat of 20 W/m^2 is applied on a 1 m x 1 m square domain, where the conductive and non-conductive material thermal conductivity is given by 1 W/(m·K) and 0.001 W/(m·K), respectively. The results of this study are presented in Table 2. The topology of the GDM RM 1 design resulted in the best compliance value.

The resultant topologies and heat maps are presented in Fig. 20. The normalized temperature maps share a common color scale to facilitate visual analysis. Observe that the performance of all of the topologies changed after conversion to an explicit boundary and evaluation using commercial analysis tools. When observing the designs produced from the optimization procedures, conclusions can be drawn to explain the corresponding performance values. The poorly defined material boundaries of the homogenization approaches improve the compliance values of their respective topologies by decreasing the temperature on the domain where material is partially defined. The regular mesh designs produced by the generative algorithms also have low compliance values, but these are due to the poor capability of the coarse mesh to accurately represent the topology in a way that satisfies the volume fraction constraint. The body-fitted mesh designs have the worst compliance values, but are the most accurate when compared to the high fidelity model. Since the design representation and analysis mesh are separated, the accuracy of the FEA solution can be adjusted easily without increasing optimization problem size. A comprehensive comparison of accuracy and computational expense between all design strategies is a topic of ongoing investigation.

[1] www.inkscape.org.

Commercial FEA results can be used to compare fairly each of the design strategies. The GDM RM 1 design resulted in the best compliance value with a small margin over SIMP MMA design. Though these designs have similar compliance values, their respective structures and temperature distributions are different. While they have low compliance values, neither of these topologies result in the lowest temperature domain. A study of design objectives other than compliance, such as power density or temperature change, may reveal a different class of optimal topologies. An investigation of new topology optimization formulations, including those with temperature constraints and new objective functions, is a subject of ongoing work. While GDMs cannot exploit problem structure in the same way as established topology optimization methods such as SIMP, it is anticipated that the flexibility and targeted design exploration abilities of GDA design abstractions will enable the efficient solution of completely new problem types.

It is important to note that the space colonization GDA was specifically selected and tailored here to perform well for a specific target application. Similar results can be seen in other applications domains where generative algorithms were specifically selected to perform well for

Table 2 Compliance and maximum temperature results

Strategy	Standard		COMSOL	
	C	T_{max} [K]	C	T_{max} [K]
SIMP OC	1709	253	2650	431
Threshold	2320	335	2650	431
SIMP MMA	1857	200	2119	445
GDM RM 1	1687	325	2109	310
GDM RM 2	1850	308	2146	315
GDM BF 1	2049	257	2128	292
GDM BF 2	2341	402	2395	427

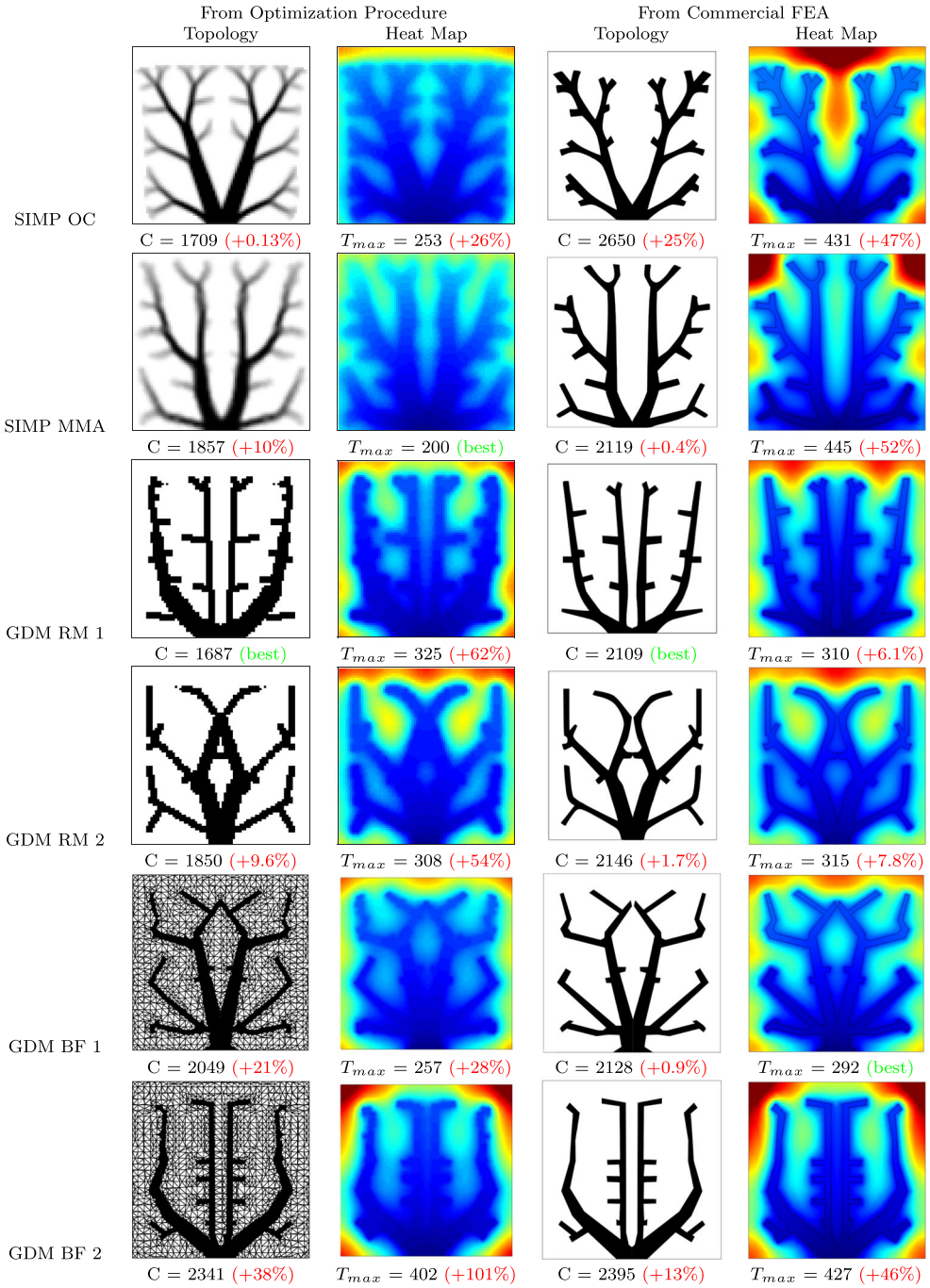

Fig. 20 Topology optimization comparison. Normalized temperatures presented are in K, and temperature maps share a common color scale

specific design problems. These applications are reviewed by Khetan et al. (2015). A fundamentally different class of thermal system designs may arise, however, from using new objective functions, which in turn may necessitate a new GDA. Current examples of successful GDMs in the literature take advantage of intuitively obvious connections between outputs of existing GDAs and engineering design problems (e.g., dendritic patterns and thermal or fluid flow problems). More general application of GDMs might be achieved through construction of custom GDAs to meet the needs of design problems for which there is no obvious connection to an existing GDA. This is a topic of ongoing study.

9 Conclusion

A method for generating dendritic topologies for heat conduction systems was presented as a design abstraction for optimization. Using a specific generative algorithm, the

space colonization algorithm, in conjunction with a genetic algorithm supported an effective search of the design space. Designs presented in Section 6 demonstrated significant variations in the dendritic structure class. Strategies for evaluating the topology using both a regularized mesh and body-fitted mesh demonstrated tradeoffs in searching for an optimal topology. The body-fitted mesh increased the computational expense of the GDM, but resulted in a more accurate solution. Six unique topologies that were generated by four different methods were evaluated using a commercial finite element solver to validate the performance of each candidate design. Both compliance values and temperature distributions were analyzed. The generative design methodology was found to produce the design with the best (lowest) thermal compliance value. The GDM BF 1 design was found to produce the design with the lowest maximum temperature. Recognizing that the least thermally-compliant structure does not result in the 'coolest' domain, several areas of future work have been identified. Specifically, an investigation is ongoing of other design formulations more closely related to electronics design, a comparison of different generative algorithms in engineering design, and the construction of custom generative algorithms for more general engineering design problems.

Acknowledgments The authors would like to acknowledge the Toyota Research Institute of North America for funding this work.

References

Bejan A, Lorente S (2006) Constructal theory of generation of configuration in nature and engineering. J Appl Phys 100(4). doi:10.1063/1.2221896

Bejan A, Dincer I, Lorente S, Miguel AF, Reis AH (2004) Porous and complex flow structures in modern technology. Springer Science. doi:10.1007/978-1-4757-4221-3

Bendsoe MP (1989) Optimal shape design as a material distribution problem. Struct Optim 1(4):193–202. doi:10.1007/BF01650949

Bendsoe MP, Kikuchi N (1988) Generating optimal topologies for structural desing using a homogenization method. Comput Methods Appl Mech Eng 71(2):197–224

Bendsoe MP, Sigmund O (2004) Topology optimization - theory, methods, and application, 2nd edn. Springer. doi:10.1007/978-3-662-05086-6

Biabanaki S, Khoei A, Wriggers P (2014) Polygonal finite element methods for contact-impact problems on non-conformal meshes. Comput Methods Appl Mech Eng 269:198–221. doi:10.1016/j.cma.2013.10.025

Biabanaki SOR, Khoei AR (2012) A polygonal finite element method for modeling arbitrary interfaces in large deformation problems. Comput Mech 50(1):19–33. doi:10.1007/s00466-011-0668-4

Bowmick S, Shontz SM (2010) Towards high-quality, untangled meshes via a force-direct graph embedding approach. Procedia Comput Sci 1(1):357–366. doi:10.1016/j.procs.2010.04.039

Brackett D, Ashscroft I, Hague R (2011) Topology optimization for additive manufacturing. In: Proceedings of the 24th solid freeform fabrication symposium, pp 6–8. http://sffsymposium.engr.utexas.edu/Manuscripts/2011/2011-27-Brackett.pdf

Bruns TH (2007) Topology optimization for convection-dominated, steady-state heat transfer problems. Int J Mass Heat Transfer 50(15–16):2859–2873. doi:10.1016/j.ijheatmasstransfer.2007.01.039

Burger FH, Dirker J, Meyer JP (2013) Three-dimensional conductive heat transfer topology optimization in a cubic domain for the volume-to-surface problem. Int J Heat Mass Transfer 67:214–224. doi:10.1016/j.ijheatmasstransfer.2013.08.015

Chan J, Fu K, Schunn C, Cagan J, Wood K, Kotovsky K (2011) On the benefits and pitfalls of analogies for innovative design: ideation performance based on analogical distance, commonness, and modality of examples. J Mech Des 133(8):081,004

Chen Y, Zhou S, Li Q (2010) Multiobjective topology optimization for finite periodic structures. Comput Struct 88:806–811. doi:10.1016/j.compstruc.2009.10.003

Christiansen AN, Nobel-Jørgensen M, Aage N, Sigmund O, Bærentzen JA (2014) Topology optimization using an explicit interface representation. Struct Multidiscip Optim 49(3):387–399. doi:10.1007/s00158-013-0983-9

Deaton J, RV G (2014) A survey of structural and multidsiplinary continuum topology optimization: post 2000. Struct Multidiscip Optim 49(1):1–38. doi:10.1007/s00158-013-0956-z

de Kruijf N, Zhou S, Li Q, Mai YW (2007) Topological design of structures and composite materials with multiobjectives. Int J Solids Struct 44:7092–7109. doi:10.1016/j.ijsolstr.2007.03.028

Dede EM (2009) Multiphysics topology optimization of heat transfer and fluid flow systems. In: Proceedings of COMSOL conference

Dede EM, Joshi SN, Zhou F (2015) Topology optimization, additive layer manufacturing, and experimental testing of air-cooled heat sink. J Mech Des 137(11):1–9. doi:10.1115/1.4030989

Errera M, Bejan A (1998) Deterministic tree networks for river frainage basins. Fractals Complex Geometry, Patterns, and Scaling in Nature and Society 6(3):245–261. doi:10.1142/S0218348X98000298

Fruchterman TMJ, Reingold EM (1991) Graph drawing by force-directed placement. Softw-Pract Exper 21(11):1129–1164. doi:10.1002/spe.4380211102

Gersborg-Hansen A, Bendsoe MP, Sigmund O (2006) Topology optimization of heat conduction problems using the finite volume method. Struct Multidiscip Optim 31:251–259. doi:10.1007/s00158-005-0584-3

Heymann D, Pence D, Narayanan V (2012) Optimization of fractal-like branching microchannel heat sink for single-phase flows. Int J Therm Sci 49(8):1383–1393. doi:10.1016/j.ijthermalsci.2010.01.015

Iga A, Nishiwaki S, Yoshimura M (2009) Topology optimization for thermal conductors considering design-dependent effects, including heat conduction and convection. Int J Mass Heat Transf 52(11–12):2721–2732. doi:10.1016/j.ijheatmasstransfer.2008.12.013

Khetan A, Lohan DJ, Allison JT (2015) Managing variable-dimension structural optimization problems using generative algorithms. Struct Multidiscip Optim 50(4):695–715. doi:10.1007/s00158-015-1262-8

Kicinger R, Arciszewski T, Jong KD (2005) Evolutionary computation and structural design: a survey of the state-of-the-art. Comput Struct 83(23):1943–1978. doi:10.1016/j.compstruc.2005.03.002

Li Q, Steven G, Xie Y, Querin O (2004) Evolutionary topology optimization for temperature reduction of heat conducting fields. Int J Heat Mass Transf 47:5071–5083. doi:10.1016/j.ijheatmasstransfer.2004.06.010

Lindenmayer A (1975) Development algorithm for multicellular organisms: a survery of L-systems. J Theor Biol 54:3–22. doi:10.1016/S0022-5193(75)80051-8

Lindsey JS, Tseng I, Fu K, Cagan J (2010) A study of design fixation, its mitigation and perception in engineering design faculty. J Mech Des 132(4). doi:10.1115/1.4001110

Meinhardt M (1976) Morphogenesis of lines and nets. Models and hypothesis. Differentiation 6 6(2):117–123. http://www.eb.tuebingen.mpg.de/fileadmin/uploads/pdf/Emeriti/Hans_Meinhardt/Old_paper_pdf/76-lines-nets.pdf

Nitin (2012) On untangled meshes via Fruchterman Reingold force directed graph embedding. In: 14th international conference on modelling and simulation, pp 39–45. doi:10.1109/UKSim.2012.15

Rodkaew Y, Siripant S, Lursinsap C, Chongstitvatana P (2002) An algorithm for generating vein images for realistic modeling of a leaf. In: Proceedings of the international conference on computational mathematics and modeling. http://www.cp.eng.chula.ac.th/piak/paper/2002/cmm2002.pdf

Runions A, Fuhrer M, Lane B, Federl P, Rolland-Lagan AG, Prusinkiewicz P (2005) Modeling and visualization of leaf venation patterns. ACM Trans Graph 24:702–711. http://algorithmicbotany.org/papers/venation.sig2005.pdf

Runions A, Lane B, Prusinkiewicz P (2007) Modeling trees with a space colonization algorithm. In: Eurographics workshop on national phenomena, pp 63–70. http://algorithmicbotany.org/papers/colonization.egwnp2007.large.pdf

Sachs T (1981) The control of patterned differentiation of vascular tissues. Adv Bot Res 6:152–262. http://algorithmicbotany.org/papers/canalisation.fsmp2004.pdf

Salakij S, Liburdy JA, Pence DV, Apreotesi M (2013) Modeling in site vapor extraction during convective boiling in fractal-like branching microchannel networks. Int J Heat Mass Transf 60:700–712. doi:10.1016/j.ijheatmasstransfer.2013.01.004

Sarhangi Fard A, Hulsen MA, Meijer HEH, Famili NMH, Anderson PD (2012) Adaptive non-conformal mesh refinement and extended finite element method for viscous flow inside complex moving geometries. Int J Numer Methods Fluids 68(8):1031–1052. doi:10.1002/fld.2595

Sigmund O, Maute K (2013) Topology optimization approaches. Struct Multidiscip Optim 48(6):1031–1055. doi:10.1007/s00158-013-0978-6

Svanberg K (1987) The method of moving asymptotes – a new method for structural optimization. Int J Numer Methods Eng 24:359–373

Svanberg K, Svard H (2013) Density filters for topology optimization based on the geometric harmonic means. In: 10th world congress on structural and multidisciplinary optimization. Orlando

Talischi C, Paulino GH, Pereira A, Menezes IFM (2012) Polymesher: a general-purpose mesh generator for polygonal element written in Matlab. Struct Multidiscip Optim 45(3):309–328. doi:10.1007/s00158-011-0706-z

Yoon GH (2010) Topological design of heat dissipating structure with Froce convective heat transfer. J Mech Sci Technol 24(6):1225–1233. doi:10.1007/s12206-010-0328-1

Zhuang C, Xiong Z, Ding H (2007) A level set method for topology optimization of heat conduction problems under multiple loading cases. Comput Methods Appl Mech Eng 196:1074–1084. doi:10.1016/j.cma.2006.08.005